The orphan nuclear receptor SHP regulates PGC-1α expression and energy production in brown adipocytes

Li Wang,[2] Jun Liu,[1] Pradip Saha,[1] Jiansheng Huang,[2] Lawrence Chan,[1] Bruce Spiegelman,[3] and David D. Moore[1,*]

[1]Department of Molecular and Cellular Biology, Baylor College of Medicine, Houston, Texas 77030
[2]Departments of Medicine and Pharmacology, The University of Kansas Medical Center, Kansas City, Kansas 66160
[3]The Dana Farber Cancer Research Institute, Boston, Massachusetts 02115
*Correspondence: moore@bcm.tmc.edu

Summary

Brown adipocytes increase energy production in response to induction of PGC-1α, a dominant regulator of energy metabolism. We have found that the orphan nuclear receptor SHP (NR0B2) is a negative regulator of PGC-1α expression in brown adipocytes. Mice lacking SHP show increased basal expression of PGC-1α, increased energy expenditure, and resistance to diet-induced obesity. Increased PGC-1α expression in *SHP* null brown adipose tissue is not due to β-adrenergic activation, since it is also observed in primary cultures of *SHP*$^{-/-}$ brown adipocytes that are not exposed to such stimuli. In addition, acute inhibition of SHP expression in cultured wild-type brown adipocytes increases basal PGC-1α expression, and SHP overexpression in SHP null brown adipocytes decreases it. The orphan nuclear receptor ERRγ is expressed in BAT and its transactivation of the PGC-1α promoter is potently inhibited by SHP. We conclude that SHP functions as a negative regulator of energy production in BAT.

Introduction

Body weight is a direct outcome of the balance of energy input and output (Lowell and Spiegelman, 2000), and recent advances have identified a number of factors that regulate the input side of this equation (Flier, 2004). Of particular importance is leptin, a satiety hormone produced by adipose tissue that acts to limit food intake. In the absence of leptin, both rodents and humans become massively obese. A number of other peripheral factors, including gut peptides such as CCK and PYY, have also been implicated in regulation of energy input (Druce et al., 2004). These factors exert many of their effects on the brain, where additional signals such as α-MSH and NPY contribute to the overall control of feeding behavior (Flier, 2004).

Energy output is also regulated. The best-understood mechanism for this is adaptive (or facultative) thermogenesis, which maintains body temperature when ambient temperatures decrease, particularly in rodents and other small mammals. This is primarily a due to increased energy output in skeletal muscle and brown adipose tissue (BAT). Muscles shiver to produce energy in response to cold. In BAT, nonshivering thermogenesis converts the energy stored in fat directly into heat in a process dependent on β-adrenergic stimulation by the sympathetic nervous system (Cannon and Nedergaard, 2004; Lowell and Spiegelman, 2000).

The transcriptional coactivator PGC-1α is a key regulator of adaptive thermogenesis in both BAT and skeletal muscle (Leone et al., 2005; Lin et al., 2004; Puigserver and Spiegelman, 2003). In BAT, PGC-1α expression is dramatically induced by adrenergic stimulation in response to cold stress (Puigserver et al., 1998). This results in increased mitochondrial biogenesis due to the function of PGC-1α as a coactivator for nuclear respiratory factor 1 (NRF-1). By acting as a nuclear receptor coactivator, PGC-1α also increases expression of the mitochondrial uncoupling protein UCP1, which creates a proton leak in mitochondria that dissipates the energy produced by oxidative metabolism. The loss of adaptive thermogenesis in BAT of UCP1 deficient mice (Enerback et al., 1997) and also PGC-1α mice (Leone et al., 2005; Lin et al., 2004) demonstrates the importance of UCP1 function in this process.

In addition to a direct inductive response to the increased levels of cAMP that result from stimulation of the β3-adrenergic receptor, UCP1 expression is regulated by several nuclear receptors. Thus, a full thermogenic response requires thyroid hormone, T_3, which can be locally produced in brown adipocytes from T_4 by the type II deiodinase. Recent results suggest increased T_3 levels induce UCP-1 expression via the TRβ isoform, and also stimulate adrenergic responsiveness via the TRβα1 isoform (Ribeiro et al., 2001). UCP1 expression can also be induced by the peroxisome proliferator activated receptor PPARγ and retinoic acid receptors (del Mar Gonzalez-Barroso et al., 2000; Puigserver et al., 1998).

Another nuclear receptor cofactor expressed in BAT is the unusual orphan receptor SHP, which interacts with a number of other nuclear receptors and strongly inhibits their transactivation function (e.g., Borgius et al., 2002; Johansson et al., 2000; Lee and Moore, 2002; Seol et al., 1996). This inhibition is a two-step process in which SHP both competes with coactivators (including PGC-1α [Borgius et al., 2002; Kanaya et al., 2004]) for binding to activated nuclear receptors and functions directly as a transcriptional repressor (Johansson et al., 2000; Lee and Moore, 2002; Seol et al., 1996). In the liver, SHP inhibition of LRH-1 transactivation is a central aspect of a negative feedback loop that regulates bile acid production (Kerr et al., 2002; Wang et al., 2002), and recent results indicate

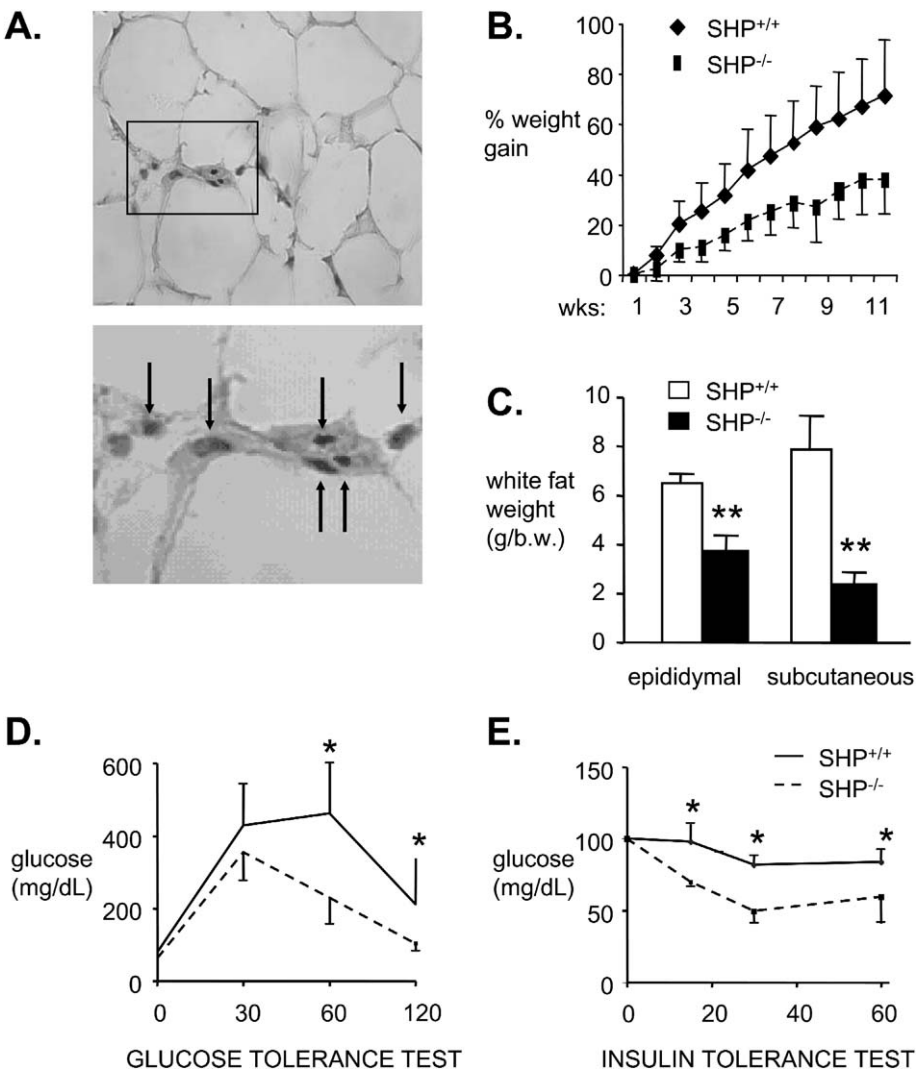

Figure 1. Resistance of *SHP* null mice to diet-induced obesity

A) Expression of SHP in white and brown adipose tissue (data not shown) was detected by immunohistochemistry with specific SHP antibodies.

B) Body weight of mice fed a high-fat diet for 12 weeks. The weight gain of the *SHP* null mice was lower than that of the wild-type mice ($p < 0.01$; n = 20/group). Values are percentage of weight gain from the starting body weight, which did not differ between wild-type and *SHP*$^{-/-}$ mice, and are expressed as the mean ± SEM.

C) Weight of epididymal and subcutaneous fat depots at the end of the high-fat diet are shown (n = 15 to 20/group). Values are expressed as the mean ± SEM. (*, $p < 0.01$; **, $p < 0.001$).

D and E) Glucose tolerance and insulin tolerance tests were performed after 12 weeks of HF diet in *SHP*$^{-/-}$ and control littermates. Values of *SHP*$^{-/-}$ mice and controls (n = 10/group) are expressed as the mean ± SEM. (*, $p < 0.01$; **, $p < 0.001$).

that SHP overexpression increases hepatic lipogenesis and triglyceride accumulation (Boulias et al., 2005).

To examine the potential role of SHP in metabolic regulatory pathways associated with obesity, *SHP* null mice were challenged with a high-fat diet. In contrast to expectations based on the association of SHP haploinsufficiency with increased body weight in humans (Nishigori et al., 2001), *SHP*$^{-/-}$ mice were resistant to diet-induced obesity. Characterization of these mice revealed increased basal PGC-1α expression in BAT and increased energy production. PGC-1α expression was also elevated in cultured *SHP*$^{-/-}$ brown adipocytes removed from potential sympathetic activation, indicating that it does not require β-adrenergic stimulation, and this was strongly confirmed by the responses of primary brown adipocytes to acutely decreased or increased SHP expression. Instead, a direct role for SHP in basal expression of PGC-1α expression was suggested by its strong inhibition of PGC-1α promoter transactivation by ERRγ, another orphan receptor expressed in BAT. These results complement previous studies suggesting inhibitory effects of SHP on PGC-1α activity (Borgius et al., 2002; Kanaya et al., 2004) and identify SHP as a novel negative regulator of energy production.

Results

Loss of SHP protects against diet-induced obesity

The initial characterization of *SHP* null mice confirmed the predicted role of this orphan in negative feedback regulation of bile acid production (Kerr et al., 2002; Wang et al., 2002) but not in other metabolic pathways as anticipated from its inhibitory effects on a number of other nuclear receptors. In particular, the body weights of *SHP*$^{-/-}$ and wild-type mice did not differ significantly on a normal-chow diet, despite the observations that SHP mRNA is expressed at low levels in white and brown adipose tissue as verified by RT-PCR analysis (data not shown) and immunohistochemistry (Figure 1A), and that SHP haploinsufficiency has been associated with modestly increased weight in Japanese populations (Nishigori et al., 2001). To further assess this potential association in mice, we challenged 8- to 9 -week-old wild-type and *SHP* null mice with a 35% (w/w) high-fat (HF) diet for 12 weeks. The *SHP*$^{-/-}$ mice

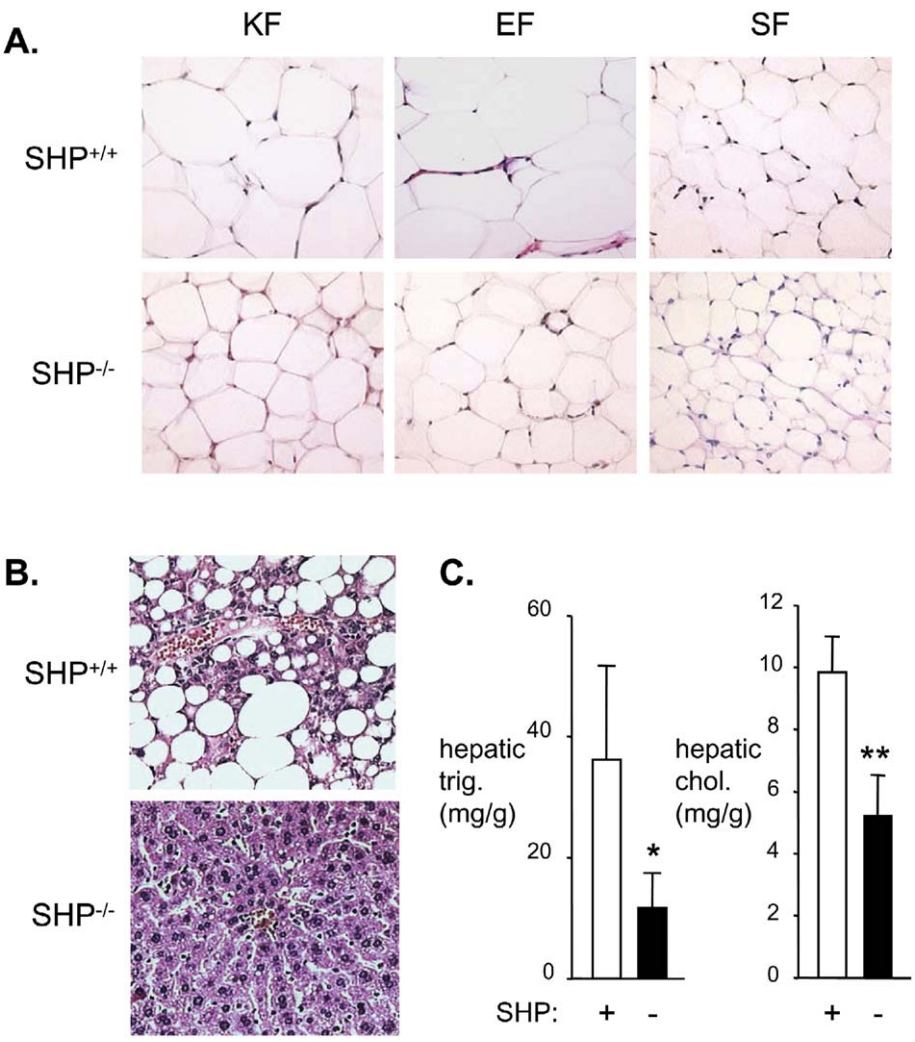

Figure 2. Decreased lipid accumulation in *SHP* null mice

A) Decreased white adipocyte cell size in kidney (KF), epididymal (EF), and subcutaneous (SF) fat in *SHP*$^{-/-}$ mice relative to wild-type mice on high-fat diet. Fat pads were collected, fixed, and subjected to hematoxylin and eosin (HE) staining (n = 3/group). A representative image is shown for each fat pad/genotype (20× magnification).

B) Livers were collected, fixed, and subjected to hematoxylin and eosin staining (n = 3/group). Representative images are shown (20× magnification). Decreased lipid accumulation was confirmed histologically by Oil Red O staining.

C) Decreased hepatic triglyceride (trig.) and cholesterol (chol.) accumulation in *SHP*$^{-/-}$ mice on high-fat diet (n = 10 to 15/group). Values are expressed as the mean ± SEM. (*, $p < 0.01$; **, $p < 0.001$).

showed blunted weight gain in response to this dietary challenge, which was evident after the first 3 weeks of feeding (Figure 1B). After 12 weeks, the wild-type mice showed 71 ± 22% weight gain, but the *SHP* null mice gained only approximately half as much, 38 ± 14%. The weight gain of the chow-fed wild-type (25%) and *SHP*$^{-/-}$ (21%) mice over the same time period was not significantly different.

The body-weight difference was largely due to a decrease in adipose tissue. Epididymal and subcutaneous fat mass was 40% and 60% lower in *SHP*$^{-/-}$ mice than in wild-type, respectively (Figure 1C). However, inguinal (kidney) fat mass was only slightly decreased (10%) in *SHP*$^{-/-}$ mice (data not shown).

The leaner *SHP*$^{-/-}$ mice showed greater insulin sensitivity. Their plasma glucose levels were 30% lower than those of the wild-type mice after a 4 hr fast but were similar to wild-type after overnight fasting. Serum insulin levels were 20% lower in the chow-fed *SHP*$^{-/-}$ mice relative to the wild-type mice and were markedly lower (70%) on the HF diet. We therefore performed glucose and insulin tolerance tests. As expected, the less obese *SHP*$^{-/-}$ mice showed relatively normal responses, while the HF fed wild-type mice showed glucose intolerance (Figure 1D) and insulin resistance (Figure 1E).

Adipocytes were enlarged in the white fat of the HF fed wild-type mice but were smaller and more heterogeneous in size in *SHP* null mice (Figure 2A), consistent with their better metabolic status. The HF diet also induced fatty liver in the wide type mice, but the livers of the HF fed *SHP*$^{-/-}$ animals contained almost no visible lipid droplets (Figure 2B), which was confirmed by marked differences in Oil Red O staining (data not shown). Consistent with this, hepatic triglyceride and cholesterol contents were significantly decreased in *SHP*$^{-/-}$ mice (Figure 2C). Hepatic free fatty acids were slightly increased, although the level did not reach statistical difference (data not shown).

Total serum triglyceride levels were not different in the wild-type and *SHP* null mice, indicating that the reduced-fat weight is not secondary to decreased lipid availability. However, total serum cholesterol levels were significantly decreased in *SHP*$^{-/-}$ mice compared with wild-type littermates (data not shown).

Loss of SHP increases thermogenesis in brown adipose tissue

Consistent with an approximately 50% decrease in serum leptin, the *SHP*$^{-/-}$ mice consume somewhat greater amounts of

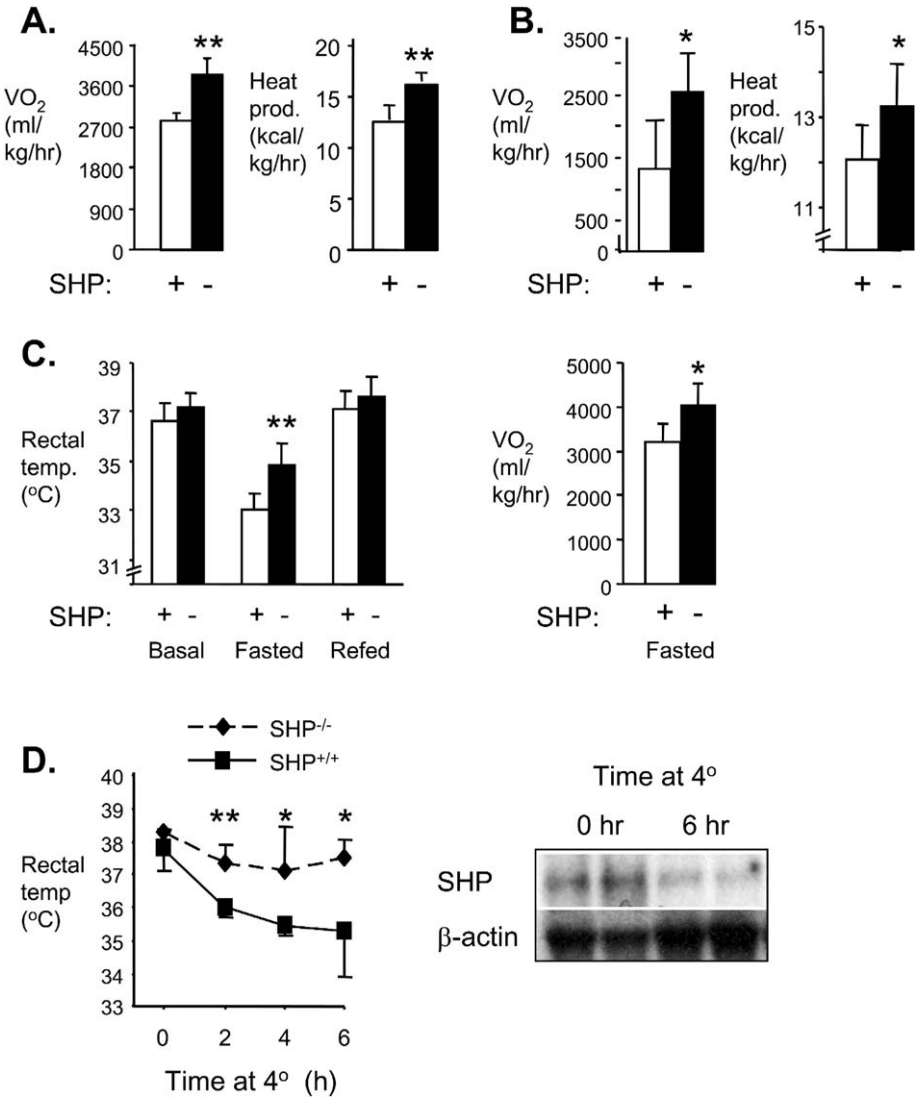

Figure 3. Increased energy expenditure in *SHP*$^{-/-}$ mice

A) Increased O_2 consumption and heat production in *SHP*$^{-/-}$ mice on high-fat diet. Mice were subjected to indirect calorimetry for 24 hr at the end of the high-fat diet period (Oxymas, Colombus Instruments) (n = 6/group). Values are expressed as the mean ± SEM. (**, $p < 0.001$).

B) Increased O_2 consumption and heat production in *SHP*$^{-/-}$ mice on normal-chow diet. 8–9 week old wild-type and *SHP*$^{-/-}$ mice were fed control chow diet for 12 weeks to match the age of the high-fat diet group. Mice were subjected to indirect calorimetry at the end of feeding (n = 6/group). (*, $p < 0.01$).

C) Rectal temperatures of chow-fed wild-type (n = 9) and *SHP*$^{-/-}$ (n = 13) mice were measured under basal conditions, after an overnight fast, and after 2 hr of refeeding, as indicated (** $p < 0.001$). Mice were subjected to indirect calorimetry for 2 hr at the end of fasting (n = 6/group) and increased O_2 consumption was observed in *SHP*$^{-/-}$ animals. Values are expressed as the mean ± SEM. (*, $p < 0.01$).

D) Resistance of *SHP*$^{-/-}$ mice to decreased body temperature subsequent to cold exposure. Rectal temperatures of chow-fed wild-type and *SHP*$^{-/-}$ mice were measured before and at increasing times after exposure to a 4°C environment. (** $p < 0.001$; * $p < 0.05$). SHP expression of wild-type mice was analyzed at 0 and 6 hr after cold exposure by Northern analysis.

the high-fat diet than the wild-type animals (data not shown). Thus, their resistance to diet induced obesity should be a consequence of increased energy expenditure. This was confirmed by a variety of both indirect and direct approaches, including analysis of oxygen consumption, CO_2 generation, heat production, and body temperature. HF-fed *SHP*$^{-/-}$ mice showed significantly higher O_2 consumption than control wild-type littermates over 24 hr (Figure 3A). Heat production (Figure 3A), CO_2 generation, and body temperature were also significantly higher in the HF fed *SHP* null mice.

Based on these results, more detailed studies on chow-fed animals revealed a lesser but significant increase in O_2 consumption and heat production in the *SHP*$^{-/-}$ mice relative to wild-type mice (Figure 3B). This was apparently balanced by a modestly increased food intake since, as previously described (Wang et al., 2002), the chow-fed *SHP*$^{-/-}$ animals did not show decreased weight.

A simple explanation for the changes in energy balance observed in the *SHP* null mice is increased thermogenesis in BAT. Although the basal body temperature of the chow-fed wild-type and *SHP* null mice did not differ, the body temperature of fasted *SHP* null mice was significantly elevated relative to wild-type and their oxygen consumption was increased (Figure 3C). Increased thermogenesis should counteract the initial decrease in body temperature associated with cold exposure, and the rate of this decrease was lower in chow-fed *SHP*$^{-/-}$ mice than in wild-type (Figure 3D). Consistent with a negative effect of SHP on thermogenesis in the wild-type mice, the induction of BAT energy production in response to 6 hr of cold exposure was associated with decreased SHP mRNA expression (Figure 3D).

As expected from the increased basal energy expenditure, the interscapular BAT of the high-fat fed *SHP*$^{-/-}$ mice was darker in color and had less surrounding WAT than that of wild-type littermates, although BAT weight was not different between the two genotypes (data not shown). There was an approximately 50% increase in cell density in *SHP* null BAT, and the *SHP*$^{-/-}$ brown adipocytes were relatively small, with smaller lipid droplets (Figure 4A). These changes in the *SHP*$^{-/-}$ BAT are not secondary consequences of the high-fat diet but are pres-

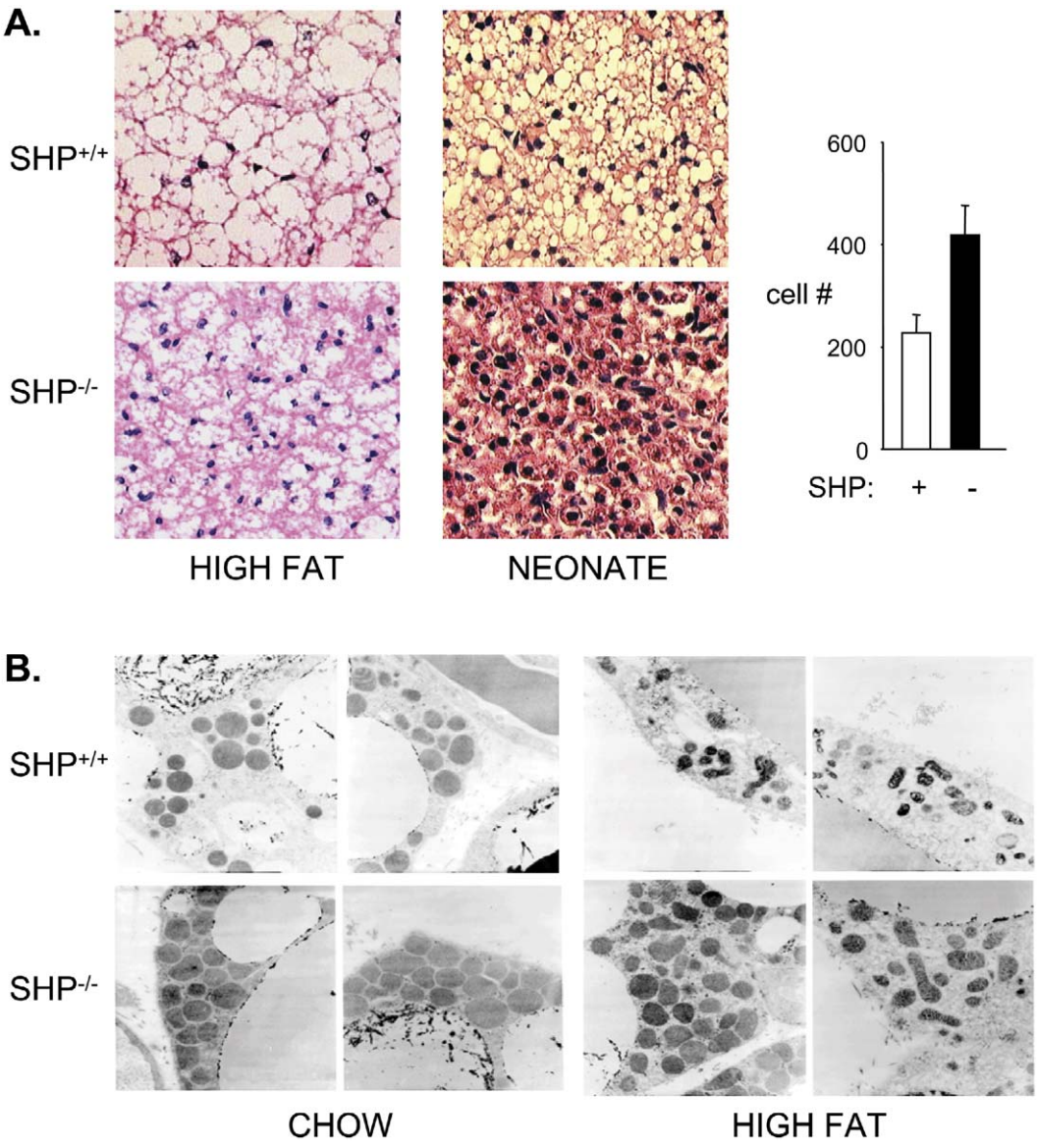

Figure 4. Alteration of BAT morphology in *SHP*$^{-/-}$ mice

A) Hematoxylin and eosin (HE) staining images of BAT from adult mice on high-fat diet or 1-day-old neonates. Similar results were observed with BAT of chow-fed adult mice BAT (data not shown). Cell density was measured by counting equal areas (n = 3/group, 20× magnification).
B) Electron microscopy of *SHP*$^{-/-}$ BAT relative to wild-type BAT on both chow (left panels) and high-fat diet (right panels). (n = 3/group, mag. × 12,000).

ent from birth, since similar differences were observed in neonatal *SHP*$^{-/-}$ mice and their wild-type siblings (Figure 4A). Electron microscopy demonstrated increased mitochondrial content in BAT of both chow and HF fed *SHP*$^{-/-}$ mice (Figure 4B).

Loss of SHP increases thermogenic gene expression in brown adipocyte

The emergence of PGC-1α as a central regulator of mitochondrial content and energy production provides a potential mechanism to account for these effects (Puigserver and Spiegelman, 2003), and normalized PGC-1α mRNA expression was 8- and 10-fold higher in *SHP* null mice than wild-type mice on the HF and chow diets (Figure 5A). PGC-1α mRNA was also increased in white adipose tissue (Figure 5B) but not in other potential direct or indirect SHP target tissues including liver, heart, and skeletal muscle (data not shown). Expression of the mitochondrial uncoupling protein UCP1 is required for increased energy production, and UCP1 mRNA expression in BAT was elevated in the *SHP*$^{-/-}$ mice on both the chow (2-fold) and HF (2.3-fold) diets. Western blotting confirmed that UCP1 protein levels were also increased (Figure 5C). Though modest, this elevation of UCP1 expression is comparable to that observed in transgenic mice expressing a constitutively active PPARδ transgene (Wang et al., 2003) and mice lacking the coactivator TIF2/SRC2 (Picard et al., 2002), both of which also show increased energy production and resistance to diet induced obesity.

Under ordinary circumstances, BAT activation is dependent on thyroid hormone (T_3), which is locally produced from circu-

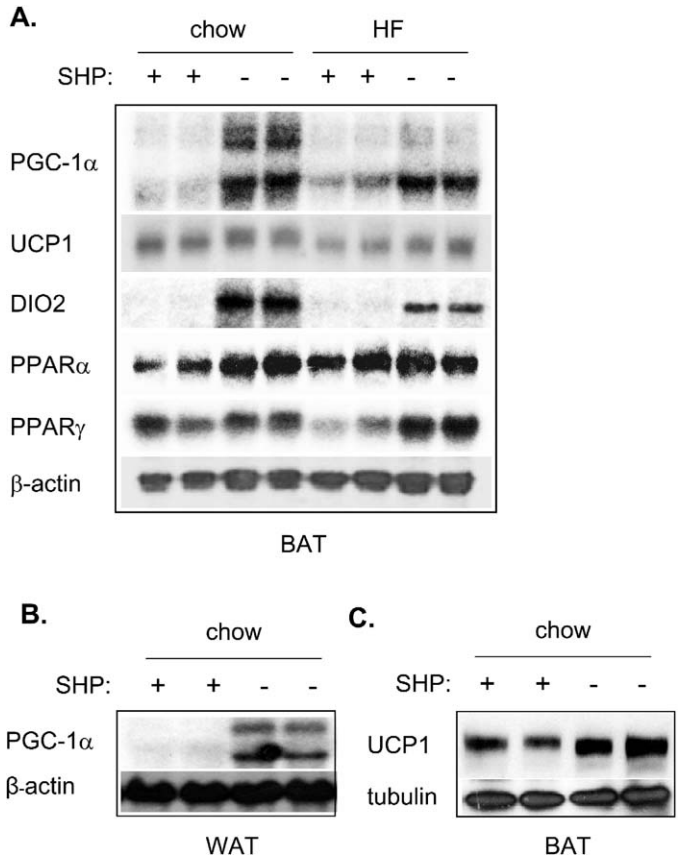

Figure 5. Alteration of BAT gene expression in *SHP*$^{-/-}$ mice

A) Expression of genes involved in BAT thermogenesis was examined by Northern blotting. BAT RNA was prepared from mice on chow or high-fat diet, and representative genes are shown. Fold increase of gene expression in *SHP*$^{-/-}$ BAT relative to wild-type BAT was determined by densitometry and normalized to β-actin.

B) Expression of PGC-1α in white fat was analyzed by Northern blotting.

C) Expression of UCP-1 protein in BAT was analyzed by Western blotting.

lating T_4 by type 2 deiodinase (Silva, 1995). DIO2 mRNA was also significantly increased in the *SHP* null BAT, particularly on the chow diet (Figure 6A). Since β-adrenergic receptor signaling is required for diet-induced thermogenesis and obesity (Bachman et al., 2002), expression of three β-adrenergic receptor isoforms was also examined, but no differences were observed (data not shown). PPARα expression in BAT was also modestly increased, especially on the chow diet, suggesting increased fatty-acid oxidation in the *SHP*$^{-/-}$ mice. In addition, hormone sensitive lipase (HSL) expression was increased about 2-fold (data not shown). Finally, PPARγ expression was also increased in *SHP*$^{-/-}$ BAT, particularly on HF diet, which may correlate with the increased insulin sensitivity of the mice.

These results raise the important question of whether the increased BAT activity is a direct consequence of the loss of SHP function in those cells or a secondary effect of the β-adrenergic stimulatory pathway. To examine their adrenergic responsiveness, wild-type and *SHP*$^{-/-}$ mice were acutely treated with the specific β3-adrenergic receptor agonist CL-214,613 (CL). We hypothesized that the effect of an additional stimulus should be blunted if the *SHP*$^{-/-}$ BAT were already subject to endogenous adrenergic activation, but no such decrease was observed. Instead, although the *SHP*$^{-/-}$ mice showed the expected higher basal levels of heat production, their induction of heat production, and oxygen consumption in response to CL-214,613 was greater than that of the wild-type animals (Figure 6A). Consistent with this, the elevated basal levels of UCP1 protein in the *SHP*$^{-/-}$ mice, which were comparable to those of the CL-214,613-treated wild-type BAT, were further increased by adrenergic stimulation (Figure 6B). As in the cold exposed wild-type mice, the increased energy production in the CL-214,613-treated wild-type BAT was associated with decreased SHP mRNA levels (Figure 6B).

Explanting and culturing the brown adipocytes provides a more direct test of the cell autonomous nature of the increased PGC-1α expression in the *SHP*$^{-/-}$ BAT, since such cells are completely removed from the potential stimulatory effects of adrenergic or other pathways. Consistent with the in vivo response to CL-214,613 stimulation, *SHP*$^{-/-}$ primary brown adipocytes were much more sensitive to the additive effect of T_3 and the β-adrenergic receptor agonist noradrenalin, as reflected by stronger induction of UCP1 mRNA (Figure 6C).

More importantly, the markedly elevated basal expression of PGC-1α in cultured *SHP*$^{-/-}$ brown adipocytes provides strong evidence for a direct inhibitory effect of SHP on PGC-1α gene expression (Figure 6D). As in the animal studies, UCP1 expression was elevated in the cultured *SHP*$^{-/-}$ brown adipocytes in the absence of any stimulation (Figure 6D). Activation of the differentiated cells by the combination of cAMP and 9-*cis*-retinoic acid significantly increased PGC-1α expression in the wild-type cells, but a more limited response was observed in the *SHP* null cells, suggesting that the absence of the repressor results in maximal PGC-1α expression. In agreement with the results with β-adrenergic receptor stimulation, the *SHP*$^{-/-}$ cells showed a remarkably robust induction of UCP1 mRNA levels in response to cAMP and 9-*cis*-retinoic acid (9-cisRA), indicating that UCP1 transcription may also be directly inhibited by SHP, which is known to repress RXR transactivation (Lee et al., 2000).

These results were confirmed using siRNA to acutely decrease SHP expression in the cultured wild-type brown adipocytes. As expected, this increased the low basal expression of both PGC-1α and UCP1, and treatment of the SHP depleted cells with cAMP and 9-*cis*-retinoic acid further increased expression of both the coactivator and its downstream target (Figure 6E). Finally, a gain-of-function approach was taken to further confirm the direct repressive effect of SHP on PGC-1α expression. *SHP* null primary brown adipocytes were transduced with an SHP expressing adenovirus or control virus. This strong SHP overexpression decreased PGC-1α expression to undetectable levels (Figure 6F). Treatment with cAMP and 9-*cis*-retinoic acid brought the repressed PGC-1α expression back to control level. The dramatic elevation of UCP1 expression in response to cAMP and 9-*cis*-retinoic acid in GFP infected cells was also significantly blunted upon overexpression of SHP.

Overall, these results demonstrate that loss of SHP function increases PGC-1α expression in the absence of any adrenergic stimuli and SHP overexpression inhibits it. Alterations of SHP also affect basal and especially stimulated expression of UCP1, indicating that it may also be a direct target of SHP negative regulation.

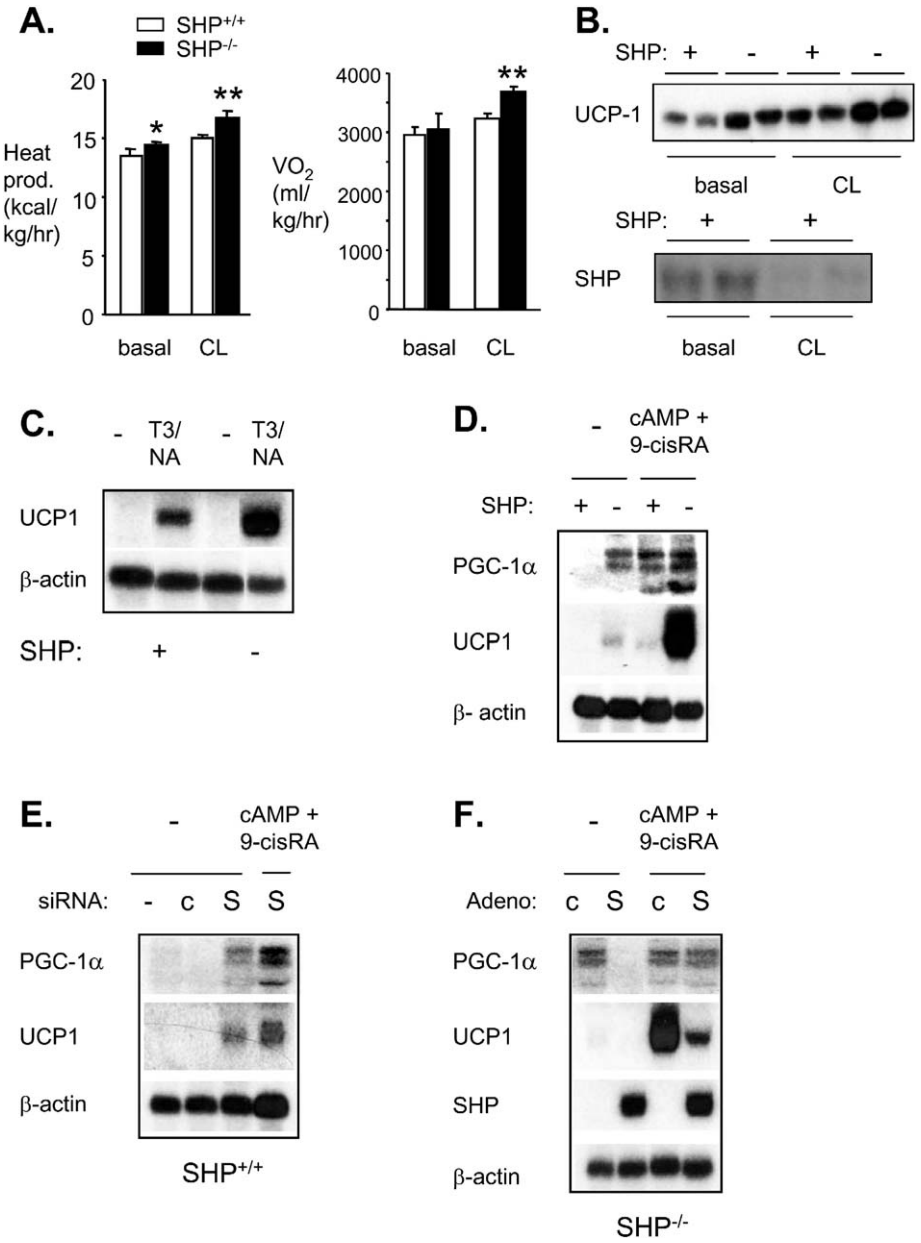

Figure 6. Cell autonomous function of SHP in BAT

A) Increased heat production and O_2 consumption in *SHP*$^{-/-}$ mice pretreated for one hour with the β3-adrenergic agonist CL-316243 (CL) and analyzed for 2 subsequent hr.

B) Expression of UCP-1 protein and SHP mRNA was analyzed in control and CL-316243 treated wild-type and SHP$^{-/-}$ BAT.

C) Increased sensitivity of UCP1 to additive T3 and noradrenaline (NA) in *SHP*$^{-/-}$ primary BAT adipocytes. Undifferentiated wild-type and *SHP* null primary BAT adipocytes were serum starved, then treated with T3 and NA for 24 hr. UCP-1 gene expression was analyzed by Northern blotting.

D) Upregulation of PGC-1α and UCP1 in *SHP*$^{-/-}$ primary BAT adipocytes. Differentiated wild-type and *SHP*$^{-/-}$ primary BAT adipocytes were untreated or treated with cAMP/9-cisRA for 6 hr and 24 hr, respectively, and PGC-1α and UCP1 gene expression was analyzed by Northern blotting.

E) Knockdown of SHP expression increases PGC-1α and UCP1 gene expression. Wild-type primary BAT adipocytes were grown to confluence, then transfected with SHP siRNA (S) or control GFP siRNA. Cells were differentiated and treated with or without cAMP/9-cisRA as in C. PGC-1α and UCP1 gene expression was analyzed by Northern blotting; SHP expression was analyzed by RT-PCR.

F) Overexpression of SHP decreases PGC-1α and UCP1 gene expression. *SHP*$^{-/-}$ primary BAT adipocytes were grown to confluence and then infected with a SHP-expressing adenovirus (S) or a control virus expressing GFP (c) for 2 hr at a multiplicity of infection of 20. Cells were differentiated and treated with or without cAMP/9-cisRA as in C. PGC-1α, UCP1, and SHP gene expression was analyzed by Northern blotting.

SHP represses ERRγ transactivation of the PGC-1α promoter

To explore the potential molecular basis for the inhibition of PGC-1α expression by SHP, BAT was screened for expression of potential SHP nuclear receptor targets. The orphan receptor ERRγ was identified as a candidate and, in transient transfections, was found to transactivate an approximately 2 kb PGC-1α promoter construct (Figure 7A). This transactivation was strongly and dose dependently inhibited by SHP coexpression, with the highest amount of SHP expression vector decreasing PGC-1α promoter activity below the basal level observed without ERRγ (Figure 7A).

The PGC-1α promoter includes several potential matches to ERRγ consensus sites, including two identical nonamers between –1769 and –1761, and –203 to –195, relative to the transcription start site. Electrophoretic mobility shift analysis confirmed that ERRγ efficiently bound these sites (Figure 7B), while several other potential sites showed lower affinity. The functionality of the proximal –203 to –195 site was confirmed by the strong transactivation of a smaller –250 PGC-1α promoter construct by ERRγ and the absence of such a response in an appropriate mutant derivative (Figure 7C). In contrast, ERRγ responsiveness was retained in a mutant –2000 promoter construct lacking the proximal site but retaining the distal –1769 and –1761 element, indicating this upstream site or possibly other elements contribute to the overall responsiveness of the full promoter. These results predict that SHP should be recruited to the PGC-1α promoter, and this was confirmed in the mouse HIB1B brown adipose cell line using chromatin immunoprecipitation with a SHP antibody and primers flanking the proximal

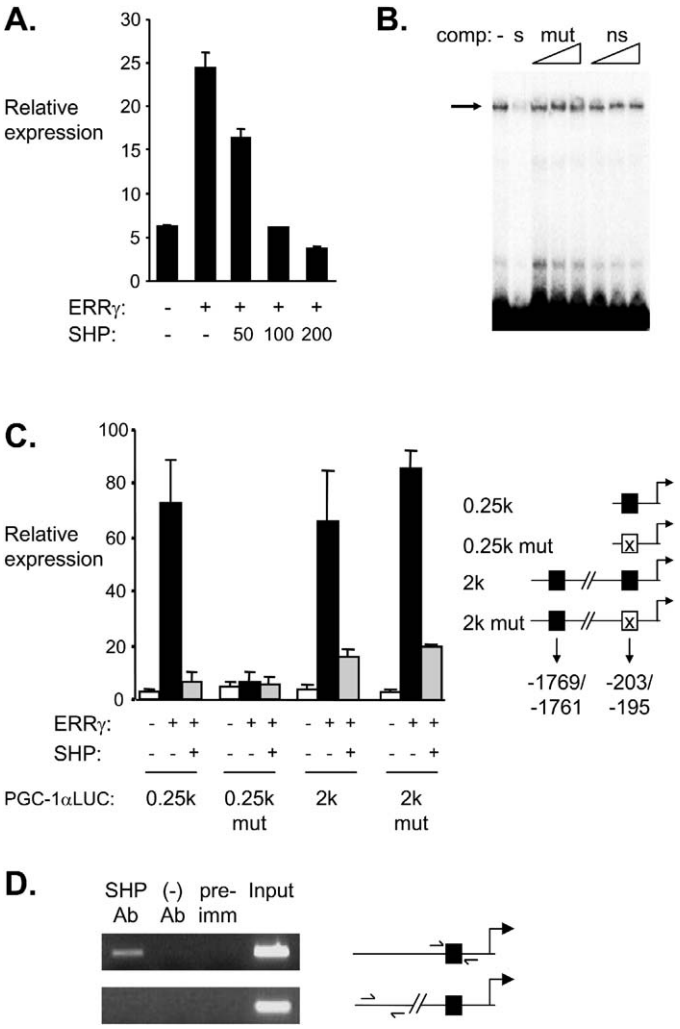

Figure 7. SHP represses ERRγ transactivation of the PGC-1 α promoter

A) SHP represses promoter activity of PGC-1α by ERRγ in a dose-dependent manner. Cells were transiently transfected with a reporter construct containing 2 kb of mPGC-1α promoter fused to luciferase together with an ERRγ expression vector in the absence or presence of an SHP expression vector. Similar results were obtained with a series of 5′ deletions of the mPGC-1α promoter (6K, 4K, 2K, 0.9K, and 0.25K) and in either Hela cells or in the brown fat-derived cell line HIB1B.

B) Specific binding of ERRγ to the potential ERRγ binding site located between –203 to –195 in the proximal mPGC-1α promoter. ERRγ was in vitro translated, and DNA binding was assayed in buffer containing ^{32}P-labeled probe, together with competitor oligonucleotides: s (self), mut (mutant self), and ns (nonspecific). DNA-protein complexes were resolved by electrophoresis in 6% native acrylamide gels and visualized by autoradiography.

C) Mutagenesis of the mPGC-1α promoter. The –203 to –195 ERRγ site was mutated using PCR-based site-directed mutagenesis. Transient transfections were performed with indicated PGC-1α promoter Luc constructs together with ERRγ (100 ng) expression vector in the absence or presence of SHP expression vector (100 ng). Luciferase activity was measured and normalized against β-galactosidase activity.

D) Chromatin immunoprecipitation. Crosslinked chromatin was precipitated with anti-SHP, preimmune, or with no antisera, using primers amplifying the proximal ERRγ binding site or an upstream sequence, as indicated.

ERRγ binding site (Figure 7D). No binding was observed to an upstream flanking fragment. Overall, we conclude that the PGC-1α promoter can be potently transactivated by ERRγ and that this response can be reversed by SHP.

Discussion

Much of the recent insight into the molecular basis for maintenance of energy balance has been based on brain pathways that modulate energy input (Flier, 2004), but energy output is also a key factor in determining body weight. The best-studied mechanism for regulation of energy production is adaptive thermogenesis, which allows rodents and other small mammals to maintain body temperature in cold environments (Cannon and Nedergaard, 2004; Lowell and Spiegelman, 2000). The results described here identify SHP as a potential negative regulator of energy expenditure in BAT.

This contrasts with the reported association of SHP haploinsufficiency with increased body weight in Japanese (Nishigori et al., 2001) and a possible link between decreased SHP activity and body weight in European populations (Hung et al., 2003; Mitchell et al., 2003). However, such differences are consistent with several other examples of divergent effects of loss of nuclear receptor function in humans and rodents. For example, heterozygous loss of function of PPARγ in mice (Miles et al., 2000) increases insulin sensitivity, while humans with a single dominant negative allele have severe insulin resistance (Barroso et al., 1999). Phenotypic discrepancies are also evident for HNF-4α (Watt et al., 2003; Yamagata et al., 1996), SF-1 (Achermann et al., 1999) and SHP's closest relative, DAX-1 (Yu et al., 1998). In many of these cases, including SHP, phenotypic differences may be due to dominant negative effects of the human alleles not shared by the murine null alleles. In addition, the metabolic effects of a particular gene can be modified by the effects of other genes, and there are obviously myriad variations between the murine and human backgrounds. The potential importance of such modifier effects is supported by preliminary analysis of mice carrying the *SHP*$^{-/-}$ allele in a pure C57/Bl6 background, which show a more limited increase in BAT PGC-1α expression than that observed in the 129/SvJ × C57/Bl6 mixed background animals described here.

Adaptive thermogenesis in BAT allows rodents to slow the development of obesity when overfed and maintain body temperature in cold environments (Cannon and Nedergaard, 2004; Lowell and Spiegelman, 2000). Although BAT has generally not been thought to play a significant role in this process in humans, it is important for thermoregulation in human neonates and could be relevant in adults in several circumstances, including activation of the β3-adrenergic receptor (Fisher et al., 1998; van Baak et al., 2002). Consistent with this, overexpression of PGC-1α in human white adipocytes confers several brown adipocyte specific features, including UCP-1 expression and increased fatty-acid oxidation (Tiraby et al., 2003). These results suggest that increasing PGC-1α expression in human white adipose tissue, possibly by decreasing SHP activity as observed in the SHP$^{-/-}$ mice (Figure 5B), could have beneficial effects on obesity.

The increased PGC-1α expression observed in BAT of both chow and HF fed *SHP* null animals is also observed in primary brown adipocytes. Since these cultured cells are not subject to β-adrenergic activation, we conclude that the increased PGC-1α expression must be a cell autonomous consequence of the loss of SHP function in BAT. SHP is coexpressed in BAT with the orphan receptor ERRγ, which can potently stimulate PGC-1α promoter activity. Both the current and previous results (Sanyal et al., 2002) show that SHP strongly inhibits ERRγ

transactivation. Thus, the loss of this SHP repression likely contributes to the increased basal BAT PGC-1α expression in the *SHP* null BAT. The marked superinduction of UCP1 expression in *SHP*$^{-/-}$ primary brown adipocytes in response to cAMP and 9-*cis*-retinoic acid suggests that UCP1 may also be a direct target of negative regulation by SHP. Both the previously reported repression of RXR transactivation by SHP (Lee et al., 2000) and the increased thermogenesis observed in the *SHP* null animals treated with the β3-adrenergic receptor CL-214,613 are consistent with this possibility.

Loss of SHP does not lead to increased PGC-1α expression in other potential metabolic target tissues. This may be due to differential expression of factors that regulate SHP expression, including ERRγ. Thus, while SHP expression is high in liver (Seol et al., 1996), where PGC-1α functions in glucose metabolism (Rhee et al., 2003; Yoon et al., 2001), ERRγ expression is very low (Sanyal et al., 2002). Basal hepatic PGC-1α expression is apparently not dependent on ERRγ, HNF-4α (Rhee et al., 2003) or other transcription factors inhibited by SHP such as LRH-1. The situation is reversed in skeletal muscle, where ERRγ is expressed at a low level but SHP expression is absent (Sanyal et al., 2002).

Increases in energy dissipation and resistance to obesity similar to those described here were observed in mice that either lack the nuclear receptor coactivator TIF2/SRC2 (Picard et al., 2002) or express a VP16-PPARδ fusion protein in adipose tissue (Wang et al., 2003). A specific increase in BAT UCP1 by a quite different mechanism also confers resistance to obesity (Zhou et al., 2003). Thus, increased thermogenesis in BAT presumably contributes to the increased energy output in the three nuclear receptor/coactivator mouse models, although preliminary results also indicate a modest increase in spontaneous motor activity in the *SHP* null mice and more detailed studies will be required to characterize the role of BAT and other potential targets in overall energy balance in these mice. Like the TIF2/SRC2 knockouts and VP-16/PPARδ transgenics, however, the *SHP* null mice showed no alterations in expression of PGC-1α or other relevant target genes in skeletal muscle, another potential thermogenic tissue. As reported for the TIF2/SRC2 null mice, the SHP deficient animals also showed no changes in serum levels of thyroid hormone or other potential metabolic activators.

Distinct molecular mechanisms that converge on PGC-1α activity may account for the increased BAT activity in the three strains. In the case of the *SHP*$^{-/-}$ mice, we propose that increased expression of PGC-1α and possibly also UCP1 is a direct consequence of the loss of this negative nuclear receptor cofactor. Since TIF2/SRC2 negatively regulates PGC-1α function by blocking the potent synergizing effects of its relative SRC1, the loss of this coactivator also increases PGC-1α activity (Picard et al., 2002). Although there was no evidence for increased PGC-1α expression or function in the VP16-PPARδ transgenics (Wang et al., 2003), PGC-1α is a PPARδ coactivator and it is reasonable to assume that the heterologous transcriptional activation domain would have similar positive effects on appropriate target genes. While the obvious differences in the mechanisms of activation presumably result in significant variations, it will be interesting to test the prediction that further characterization of these three mouse models of obesity resistance will reveal more common phenotypes and further insights into energy balance.

Experimental procedures

Mouse studies

SHP$^{-/-}$ mice were previously described (Wang et al., 2002) and were maintained on a C57BL6/129sv hybrid background. Age-matched groups of 2- to 3-month-old SHP$^{+/+}$ and SHP$^{-/-}$ siblings derived from heterozygous intercrosses of SHP$^{+/-}$ were used in the experiments. Unless otherwise indicated, mice were housed 5 per cage in temperature controlled (23°C) virus-free facilities on a 12 hr light/dark cycle (07:00 on–19:00 off) and fed a standard rodent chow (test diet no. 5001, 4% [w/w] fat, Harlan Teklad Diets) and water ad libitum. Age- and sex-matched groups of 8- to 9-week-old wild-type and *SHP*$^{-/-}$ mice were used in all the experiments. All protocols for animal use and euthanasia were approved by the Animal Care Committee at Baylor College of Medicine and were in accordance with National Institutes of Health guidelines.

Mice on a high-fat diet were fed chow containing 35.9% fat (Harlan Teklad Diets) for 12 weeks. High-fat chow has a total energy content of 23.4kj/g, standard diet 12.6kj/g. On the day before sacrifice, mice were fasted overnight (15 hr), and blood was collected from the orbital plexus after mice were anaesthetized with avertin. Liver and fat tissues were removed for histological analysis. Tissues not used for histology were weighed, sectioned, and snap frozen in liquid nitrogen and stored at –80°C until use.

Histology and immunohistochemistry

Liver was fixed in 4% formaldehyde, dehydrated, embedded in paraffin and sectioned (4 μm). Sections were stained with Harris hematoxylin and eosin (Sigma). For Oil Red O staining, frozen tissue sections were used. Sections were examined under bright-field microscopy with an Olympus model BX50 photomicroscope.

Brown adipose tissue was isolated from the back of 8-week-old C57BL/6J wild-type and *SHP*$^{-/-}$ mice, and paraffin-embedded sections were prepared. For immunostaining, sections were deparaffinized in xylene 10 min, three times; rehydrated by immersing in a graded alcohol series (100% × 3, 95% × 3, 85% × 1, 70% × 1, respectively), 5 min for each step, immersed in running water for 5 min; boiled in preboiled 10 mM sodium citrate (pH 6.0) for 20 min for antigen retrieval; cooled to room temperature for 20 min, immersed in PBST for 1 min; incubated with 1% H_2O_2 in methanol for 15 min at room temperature to block endogenous peroxidase, washed with PBST (5 min × 3), and blocked in 10% normal goat serum (NGS) for 30 min at room temperature. Slides were incubated with a 1:50 dilution of rabbit primary antibody against human SHP (LS-A5395, Lifespan) at 4°C overnight, washed with PBST (5 min × 3), incubated with biotinylated goat anti-rabbit IgG (Zymed) for 20 min at room temperature, washed with PBST (5 min × 3), incubated in alkaline phosphatase streptavidin (Zymed) for 20 min at room temperature, washed with PBST (5 min × 3), developed with the chromagen substate (Zymed) for 10 min, rinsed with distilled water, counterstained with hematoxylin, and finally mounted in GVA mount.

RNA analysis

Total RNA was isolated from different tissues as indicated using Tri-reagent (Invitrogen) according the manufacturer's instruction. For Northern blot analysis, 10 or 20 μg of RNA was denatured, electrophoresed, transferred to nylon membrane, and probed with different cDNA probes. RNA samples were processed as previously described (Wang et al., 2002). As also described (Wang et al., 2002), all cDNA probes used in this study were prepared by RT-PCR using appropriate primers that are available upon request.

Plasma and tissue chemistry

Serum was prepared from whole blood by centrifugation at 1200 × g for 10 min using Microtainer serum separator tubes (Terumo Medical Corp.) and frozen in aliquots and stored at –20°C. Enzymatic assay kits were used for the determination of serum nonesterified fatty acids (NEFA C), glucose, cholesterol, and total triacylglycerol (Sigma). Serum insulin was measured using radioimmunoassay (Crystal Chem, Inc.).

To extract lipids, 100 mg of liver was homogenized in chloroform:methanol (2:1) and centrifuged. The lower phase containing the lipid was dried completely under a stream of N_2 and resuspended uniformly in PBS-Triton

X-100 solution by ultrasonication. Hepatic triacylglycerol, cholesterol, and free fatty-acid concentrations were determined as for the serum samples.

Glucose tolerance tests (GTT) were performed on animals that had been fasted overnight for 16 hr, whereas insulin tolerance tests (ITT) were performed on animals fasted for 4 hr in the morning. Animals were injected with either 2 g/kg body weight of glucose or 0.75 U/kg body weight of human insulin (Eli Lilly) into the peritoneal cavity. Glucose levels were measured from blood collected from the tail immediately before and 30, 60, 120 min (for GTT) or 15, 30, 60 min (for ITT) after the injection using one-touch blood glucose strips (Fastake, Life Scan).

Oxygen consumption

Oxygen consumption was assessed individually in mice fed a regular chow or a 35% fat diet using a computer-controlled open-circuit indirect calorimetry (Oxymas, Colombus Instruments) with an air flow of 0.5 l/min and a RT of 23°C. After 30 min for adaptation to the metabolic chamber, VO_2, VCO_2, and heat production were assessed at 5 min intervals for a 20–24 hr period. Mice had free access to water under fasting condition during the 12 hr light and 12 hr night period. Total oxygen consumption represents the mean of all samples collected during the experiment.

For testing the effect of β-adrenergic activation, mice were introduced into the calorimetry chamber for 3 hr to collect baseline data, and then were intraperitoneally injected with the β3-adrenergic receptor-specific agonist CL-316243 (1 mg/kg body weight). After 1 hr, O_2 consumption and heat production were measured for 2 hr.

Electron microscopy

Brown adipocyte tissues from wild-type and *SHP* null mice were fixed with 2% glutaraldehyde in PBS overnight at 4°C and then postfixed in 1% osmium tetroxide in phosphate buffer 0.1 M (pH 7.4), dehydrated in ethanol, and embedded in an Epon-Araldite mixture. Thin sections were obtained with a MT-X ultramicrotome. Electron microscopy image analysis was performed by Dr. Milton Finegold and Jim Barrish in the Gulf Coast Digestive Disease Center Core Morphology Laboratory at Texas Children's Hospital in Texas Medical Center in Houston.

Primary cell culture

Brown adipocyte progenitors were isolated from interscapular BAT of 3-4 wk old wild-type and *SHP* null mice by collagenase disaggregation as described (Cannon and Nedergaard, 2001) with minor modifications and assistance from Dr. Sheila Collins (Duke University Medical Center, Durham, NC). Primary cells were grown in DMEM supplemented with 10% FBS, 100U penicillin, 100 μg/ml streptomycin, 0.14 μg/ml fungizone, 17 μM D-pantothenic acid, 33 μM D-biotin, 100 μM ascorbic acid and 4 nM insulin. The medium was changed 1 day after plating and after 3 days cells were cultured in differentiation medium containing 50 nM insulin, 50 nM T3 and 1 μM rosiglitazone for 7 days. Differentiated brown adipocyte cultures were used for ligand treatment. 1 μM of 9-cisRA and 1 mM of 8-Br-cAMP were added to cells for 24 hr or 6 hr, respectively, before the end of culture. For checking the additive effect of thyroid hormone and β-adrenergic signaling, freshly isolated brown adipocyte cells were grown in growth medium to confluence, and were then serum starved for 24 hr. Cells were further cultured in charcoal stripped serum medium and treated with T3 and noradrenaline (NA) at the final concentration of 10 nM and 1μM, respectively, for 24 hr. RNA was isolated for Northern blotting. For all primary cultures, cells were pooled from 4–15 mice for each experiment.

Adenoviral transduction

Recombinant adenovirus vectors for expression of mPGC-1α, mSHP and the GFP control were prepared as described (Rhee et al., 2003). Viral supernatants were generated by standard methods at Baylor College of Medicine BCM virus Core facility with the assistance of Dr. Kazuhiro Oka. *SHP*$^{-/-}$ primary brown adipocytes were isolated as described above and cultured to 70%–80% confluence. They were plated at 2×10^6 per 10 cm dish and infected the next day with viral supernatant at different multiplicities of infection for 2 hr. Virus containing media were removed and cells were continuously cultured to induce differentiation, then treated with ligands as indicated above.

RNA interference

SHP siRNA was generated by using Dicer siRNA generation kit according to the manufacture's instruction (Gene Therapy systems, Inc.). Wild-type primary brown adipocytes were isolated and cultured until 70%–80% confluence. SiRNA for SH was then transfected into the cells according the manufacture's instruction (Gene Therapy systems, Inc.). Cells were then induced to differentiate and treated with ligand as indicated above.

Transient transfection and luciferase assays

Hela or H1B1B cells were maintained in Dulbecco's Modified Eagle's Medium in the presence of 10% fetal bovine serum. mPGC-1α promoter 6K, 4K, and 2K Luc constructs were as described (Handschin et al., 2003). Two additional deletion constructs of mPGC-1α promoter 0.9K and 0.25K were generated using two upstream primers: sense, 5′-GCGGGGTACCGCTTTACAAGGAGCAAGGCAAACTGCAG-3′ and 5′-GCGGGGTACCCACTGAGGCAGAGGGCTGCCTTGGAG-3′; and a common antisense primer, 5′-GCGGCTCGAGATCCACTCTGACACACAGCACACACTCATG-3′. Mutagenesis of the 0.25K construct was performed with the Exsite PCR-based site directed mutagenesis (Stratagene), and all mutations were checked by sequencing. SHP and ERRγ gene expression vectors were obtained from Dr. Yoonkwang Lee. For luciferase assays, cells were plated in 24-well plates one day before transfection, and transfections were carried out using calcium phosphate. Total DNA in each transfection was adjusted by adding appropriate amounts of pcDNA3 vector. Approximately 48 hr posttransfection, cells were harvested, and luciferase activity was measured and normalized against β-galactosidase activity as an internal control with a Dual-Luciferase Reporter System (Promega) in a Lumat LB9501 luminometer (Berthold, Wildbad, Germany). The transfection experiments were carried out independently 3 times with similar efficiency and one representative result is shown.

In vitro translation and DNA binding analysis

In vitro translated proteins were prepared by using a coupled transcription and translation kit (Promega). The efficiency of ERRγ translation was determined by a reaction containing [^{35}S] methionine, followed by SDS/PAGE and Western blotting. For protein-DNA interaction, in vitro-translated ERRγ was incubated with the following ^{32}P-labeled duplex oligonucleotide probe: wt: 5′-TTGTGCAGCAAGCTTGCACAGGA. Mutant probe: 5′- TTGTGCAGGATCCTTGCACAGGA was used as competitor. The wild-type and mutant potential ERRγ binding sequences are underlined. The binding reactions contained 30,000 cpm of ^{32}P-labeled DNA and were incubated for 30 min. with the in vitro translated proteins in 20 mM Hepes (pH 7.9), 75 mM NaCl, 1 mM dithiotreitol, 2 mM $MgCl_2$, 10% (vol/vol) glycerol/0.1 mg of BSA/10 μg/ml salmon sperm DNA. Competitor oligonucleotides were included at a 10- to 100-fold molar excess as indicated. DNA-protein complexes were resolved by electrophoresis in 6% native acrylamide gels and visualized by autoradiography.

Statistics

Data were analyzed using one-way ANOVA, followed by student's t test. $p < 0.05$ was considered significant.

Acknowledgments

We are grateful to Dr. Sheila Collins for assistance with isolation and culture of primary brown adipocytes, Dr. Milton Finegold for assistance with electron microscopy, Dr. Kazuhiro Oka for assistance in generating adenovirus stocks, and Dr Yoonkwang Lee for support and helpful discussions. This work was supported by National Institutes of Health grants R01 DK53366 and P01 DK57743 to D.D.M.

Received: May 25, 2005
Revised: August 8, 2005
Accepted: August 25, 2005
Published: October 11, 2005

References

Achermann, J.C., Ito, M., Ito, M., Hindmarsh, P.C., and Jameson, J.L. (1999). A mutation in the gene encoding steroidogenic factor-1 causes XY sex reversal and adrenal failure in humans. Nat. Genet. *22*, 125–126.

Bachman, E.S., Dhillon, H., Zhang, C.Y., Cinti, S., Bianco, A.C., Kobilka, B.K., and Lowell, B.B. (2002). betaAR signaling required for diet-induced thermogenesis and obesity resistance. Science *297*, 843–845.

Barroso, I., Gurnell, M., Crowley, V.E., Agostini, M., Schwabe, J.W., Soos, M.A., Maslen, G.L., Williams, T.D., Lewis, H., Schafer, A.J., et al. (1999). Dominant negative mutations in human PPARgamma associated with severe insulin resistance, diabetes mellitus and hypertension. Nature *402*, 880–883.

Borgius, L.J., Steffensen, K.R., Gustafsson, J.A., and Treuter, E. (2002). Glucocorticoid signaling is perturbed by the atypical orphan receptor and corepressor SHP. J. Biol. Chem. *277*, 49761–49766.

Boulias, K., Katrakili, N., Bamberg, K., Underhill, P., Greenfield, A., and Talianidis, I. (2005). Regulation of hepatic metabolic pathways by the orphan nuclear receptor SHP. EMBO J. *24*, 2624–2633.

Cannon, B., and Nedergaard, J. (2001). Cultures of adipose precursor cells from brown adipose tissue and of clonal brown-adipocyte-like cell lines. Methods Mol. Biol. *155*, 213–224.

Cannon, B., and Nedergaard, J. (2004). Brown adipose tissue: function and physiological significance. Physiol. Rev. *84*, 277–359.

del Mar Gonzalez-Barroso, M., Pecqueur, C., Gelly, C., Sanchis, D., Alves-Guerra, M.C., Bouillaud, F., Ricquier, D., and Cassard-Doulcier, A.M. (2000). Transcriptional activation of the human ucp1 gene in a rodent cell line. Synergism of retinoids, isoproterenol, and thiazolidinedione is mediated by a multipartite response element. J. Biol. Chem. *275*, 31722–31732.

Druce, M.R., Small, C.J., and Bloom, S.R. (2004). Gut Peptides regulating satiety. Endocrinology *145*, 2660–2665.

Enerback, S., Jacobsson, A., Simpson, E.M., Guerra, C., Yamashita, H., Harper, M.E., and Kozak, L.P. (1997). Mice lacking mitochondrial uncoupling protein are cold-sensitive but not obese. Nature *387*, 90–94.

Fisher, M.H., Amend, A.M., Bach, T.J., Barker, J.M., Brady, E.J., Candelore, M.R., Carroll, D., Cascieri, M.A., Chiu, S.H., Deng, L., et al. (1998). A selective human beta3 adrenergic receptor agonist increases metabolic rate in rhesus monkeys. J. Clin. Invest. *101*, 2387–2393.

Flier, J.S. (2004). Obesity wars: molecular progress confronts an expanding epidemic. Cell *116*, 337–350.

Handschin, C., Rhee, J., Lin, J., Tarr, P.T., and Spiegelman, B.M. (2003). An autoregulatory loop controls peroxisome proliferator-activated receptor gamma coactivator 1alpha expression in muscle. Proc. Natl. Acad. Sci. USA *100*, 7111–7116.

Hung, C.C., Farooqi, I.S., Ong, K., Luan, J., Keogh, J.M., Pembrey, M., Yeo, G.S., Dunger, D., Wareham, N.J., and O'Rahilly, S. (2003). Contribution of variants in the small heterodimer partner gene to birthweight, adiposity, and insulin levels: mutational analysis and association studies in multiple populations. Diabetes *52*, 1288–1291.

Johansson, L., Bavner, A., Thomsen, J.S., Farnegardh, M., Gustafsson, J.A., and Treuter, E. (2000). The orphan nuclear receptor SHP utilizes conserved LXXLL-related motifs for interactions with ligand-activated estrogen receptors. Mol. Cell. Biol. *20*, 1124–1133.

Kanaya, E., Shiraki, T., and Jingami, H. (2004). The nuclear bile acid receptor FXR is activated by PGC-1alpha in a ligand-dependent manner. Biochem. J. *382*, 913–921.

Kerr, T.A., Saeki, S., Schneider, M., Schaefer, K., Berdy, S., Redder, T., Shan, B., Russell, D.W., and Schwarz, M. (2002). Loss of Nuclear Receptor SHP Impairs but Does Not Eliminate Negative Feedback Regulation of Bile Acid Synthesis. Dev. Cell *2*, 713–720.

Lee, Y.K., Dell, H., Dowhan, D.H., Hadzopoulou-Cladaras, M., and Moore, D.D. (2000). The orphan nuclear receptor SHP inhibits hepatocyte nuclear factor 4 and retinoid X receptor transactivation: two mechanisms for repression. Mol. Cell. Biol. *20*, 187–195.

Lee, Y.K., and Moore, D.D. (2002). Dual mechanisms for repression of the monomeric orphan receptor liver receptor homologous protein-1 by the orphan small heterodimer partner. J. Biol. Chem. *277*, 2463–2467.

Leone, T.C., Lehman, J.J., Finck, B.N., Schaeffer, P.J., Wende, A.R., Boudina, S., Courtois, M., Wozniak, D.F., Sambandam, N., Bernal-Mizrachi, C., et al. (2005). PGC-1alpha deficiency causes multi-system energy metabolic derangements: muscle dysfunction, abnormal weight control and hepatic steatosis. PLoS Biol. *3*, e101. 10.1371/journal.pbio.0030101.

Lin, J., Wu, P.H., Tarr, P.T., Lindenberg, K.S., St-Pierre, J., Zhang, C.Y., Mootha, V.K., Jager, S., Vianna, C.R., Reznick, R.M., et al. (2004). Defects in adaptive energy metabolism with CNS-linked hyperactivity in PGC-1alpha null mice. Cell *119*, 121–135.

Lowell, B.B., and Spiegelman, B.M. (2000). Towards a molecular understanding of adaptive thermogenesis. Nature *404*, 652–660.

Miles, P.D., Barak, Y., He, W., Evans, R.M., and Olefsky, J.M. (2000). Improved insulin-sensitivity in mice heterozygous for PPAR-gamma deficiency. J. Clin. Invest. *105*, 287–292.

Mitchell, S.M., Weedon, M.N., Owen, K.R., Shields, B., Wilkins-Wall, B., Walker, M., McCarthy, M.I., Frayling, T.M., and Hattersley, A.T. (2003). Genetic variation in the small heterodimer partner gene and young-onset type 2 diabetes, obesity, and birth weight in UK subjects. Diabetes *52*, 1276–1279.

Nishigori, H., Tomura, H., Tonooka, N., Kanamori, M., Yamada, S., Sho, K., Inoue, I., Kikuchi, N., Onigata, K., Kojima, I., et al. (2001). Mutations in the small heterodimer partner gene are associated with mild obesity in Japanese subjects. Proc. Natl. Acad. Sci. USA *98*, 575–580.

Picard, F., Gehin, M., Annicotte, J., Rocchi, S., Champy, M.F., O'Malley, B.W., Chambon, P., and Auwerx, J. (2002). SRC-1 and TIF2 control energy balance between white and brown adipose tissues. Cell *111*, 931–941.

Puigserver, P., and Spiegelman, B.M. (2003). Peroxisome proliferator-activated receptor-gamma coactivator 1 alpha (PGC-1 alpha): transcriptional coactivator and metabolic regulator. Endocr. Rev. *24*, 78–90.

Puigserver, P., Wu, Z., Park, C.W., Graves, R., Wright, M., and Spiegelman, B.M. (1998). A cold-inducible coactivator of nuclear receptors linked to adaptive thermogenesis. Cell *92*, 829–839.

Rhee, J., Inoue, Y., Yoon, J.C., Puigserver, P., Fan, M., Gonzalez, F.J., and Spiegelman, B.M. (2003). Regulation of hepatic fasting response by PPARgamma coactivator-1alpha (PGC-1): requirement for hepatocyte nuclear factor 4alpha in gluconeogenesis. Proc. Natl. Acad. Sci. USA *100*, 4012–4017.

Ribeiro, M.O., Carvalho, S.D., Schultz, J.J., Chiellini, G., Scanlan, T.S., Bianco, A.C., and Brent, G.A. (2001). Thyroid hormone–sympathetic interaction and adaptive thermogenesis are thyroid hormone receptor isoform–specific. J. Clin. Invest. *108*, 97–105.

Sanyal, S., Kim, J.Y., Kim, H.J., Takeda, J., Lee, Y.K., Moore, D.D., and Choi, H.S. (2002). Differential regulation of the orphan nuclear receptor small heterodimer partner (SHP) gene promoter by orphan nuclear receptor ERR isoforms. J. Biol. Chem. *277*, 1739–1748.

Seol, W., Choi, H.S., and Moore, D.D. (1996). An orphan nuclear hormone receptor that lacks a DNA binding domain and heterodimerizes with other receptors. Science *272*, 1336–1339.

Silva, J.E. (1995). Thyroid hormone control of thermogenesis and energy balance. Thyroid *5*, 481–492.

Tiraby, C., Tavernier, G., Lefort, C., Larrouy, D., Bouillaud, F., Ricquier, D., and Langin, D. (2003). Acquirement of brown fat cell features by human white adipocytes. J. Biol. Chem. *278*, 33370–33376.

van Baak, M.A., Hul, G.B., Toubro, S., Astrup, A., Gottesdiener, K.M., DeSmet, M., and Saris, W.H. (2002). Acute effect of L-796568, a novel beta 3-adrenergic receptor agonist, on energy expenditure in obese men. Clin. Pharmacol. Ther. *71*, 272–279.

Wang, L., Lee, Y.-K., Bundman, D., Han, Y., Thevananther, S., Kim, C.-S., Chua, S.S., Wei, P., Heyman, R.A., Karin, M., and Moore, D.D. (2002). Redundant pathways for negative feedback regulation of bile acid production. Dev. Cell *2*, 721–731.

Wang, Y.X., Lee, C.H., Tiep, S., Yu, R.T., Ham, J., Kang, H., and Evans, R.M. (2003). Peroxisome-proliferator-activated receptor delta activates fat metabolism to prevent obesity. Cell *113*, 159–170.

Watt, A.J., Garrison, W.D., and Duncan, S.A. (2003). HNF4: a central regulator of hepatocyte differentiation and function. Hepatology *37*, 1249–1253.

Yamagata, K., Furuta, H., Oda, N., Kaisaki, P.J., Menzel, S., Cox, N.J., Fajans, S.S., Signorini, S., Stoffel, M., and Bell, G.I. (1996). Mutations in the hepatocyte nuclear factor-4alpha gene in maturity-onset diabetes of the young (MODY1). Nature *384*, 458–460.

Yoon, J.C., Puigserver, P., Chen, G., Donovan, J., Wu, Z., Rhee, J., Adelmant, G., Stafford, J., Kahn, C.R., Granner, D.K., et al. (2001). Control of hepatic gluconeogenesis through the transcriptional coactivator PGC-1. Nature *413*, 131–138.

Yu, R.N., Ito, M., Saunders, T.L., Camper, S.A., and Jameson, J.L. (1998). Role of Ahch in gonadal development and gametogenesis. Nat. Genet. *20*, 353–357.

Zhou, Z., Yon Toh, S., Chen, Z., Guo, K., Ng, C.P., Ponniah, S., Lin, S.C., Hong, W., and Li, P. (2003). Cidea-deficient mice have lean phenotype and are resistant to obesity. Nat. Genet. *35*, 49–56.